



ELSEVIER

Available online at [www.sciencedirect.com](http://www.sciencedirect.com)

SCIENCE @ DIRECT®

Applied Surface Science 210 (2003) 146–152

applied  
surface science

[www.elsevier.com/locate/apsusc](http://www.elsevier.com/locate/apsusc)

## Dependence of the tip–surface interaction on the surface electronic structure

A.S. Foster<sup>a,\*</sup>, A.Y. Gal<sup>b</sup>, Y.J. Lee<sup>a</sup>, A.L. Shluger<sup>b</sup>, R.M. Nieminen<sup>a</sup>

<sup>a</sup>Laboratory of Physics, Helsinki University of Technology, P.O. Box 1100, Helsinki 02015, Finland

<sup>b</sup>Department of Physics and Astronomy, University College London, Gower Street, London WC1E 6BT, UK

### Abstract

We compare the results of ab initio calculations of the interaction of Si tips with the surfaces of CaCO<sub>3</sub>, MgO, and CaF<sub>2</sub>. The calculations were performed using the density functional theory and the SIESTA code. We used a conventional Si tip model with a dangling bond at the apex. The results demonstrate a considerable electron density redistribution between the tip and surface, which depends on the energy offset of the Si states with respect to the occupied and empty states of the insulator. The tip–surface interaction has two main components. One is due to the polarisation of the neutral Si tip by the surface electric field. The stronger electrostatic component originates from the electron redistribution effect mentioned above. As a result the strength of the tip–surface interaction is comparable to that for ionic tips (e.g. modelled by the MgO cube).

© 2003 Elsevier Science B.V. All rights reserved.

*Keywords:* Tip–surface; Electronic structure; Si

### 1. Introduction

It is well known that the tip–surface interaction depends on the tip and surface electronic structures. However, this issue so far only been really explored in the realm of STM rather than AFM. Most AFM simulations for ionic surfaces have been performed using ionic tips, justified by the fact that commercial silicon tips are often oxidised and/or covered by the surface material. In this case the tip–surface interaction is mainly determined by the Coulomb interaction between the tip and surface [1]. On more reactive silicon surfaces it has been shown that for a pure silicon tip, image contrast is dominated by the onset of covalent bonding between dangling bonds in the tip and surface [2,3], and these forces have recently been explored in detail experimentally [4]. Similar

mechanisms have been demonstrated for surfaces of other semiconductors, such as InP [5], GaAs [6], and TiO<sub>2</sub> [7]. However, the interaction of Si or metal tips with insulating surfaces has not been studied theoretically so far.

The tip–surface interaction is closely related to the strength of adhesion between the two materials. The adhesion between metals and insulators is studied best and is known to depend on the metal electronegativity (see, for example, Refs. [8–10]). One can also expect some degree of electron transfer between the tip and surface materials dependent on the relative position of their energy bands at the interface. Indeed, the tunnelling current has been observed experimentally in STM on CaF<sub>2</sub> film grown on Si(1 1 1) at bias voltage of 3.5 eV when tip was brought into resonance with the Ca-determined CaF<sub>2</sub> conduction band states [11]. On the other hand, the onset of covalent bonding between Si and F atoms at the Si/CaF<sub>2</sub> interface has been

\* Corresponding author.

predicted theoretically [12], although the energy offset between the occupied fluorine states of  $\text{CaF}_2$  and unoccupied Si states is the largest in this case (about 8 eV experimentally and 6 eV theoretically [12]).

There have been already several studies of oxide surfaces, such as NiO, with tips covered by metals [13,14]. The use of clean silicon tips for insulating surfaces is currently difficult to prove experimentally. However, improving tip preparation techniques [15] may allow one to achieve this in the near future. To study the mechanism of contrast formation and the nature of the Si tip–surface interaction on wide-gap insulator surfaces we have considered three insulators with different bandgaps and surface structures:  $\text{CaCO}_3$ , MgO, and  $\text{CaF}_2$ . AFM imaging of these surfaces has been simulated in our previous studies using the ionic tip model [16], providing useful comparison. The current results demonstrate electron density redistribution between the tip and surface, and its dependence on the offset of the Si states with respect to the occupied and empty states of the insulator. This effect strongly contributes to the tip–surface interaction.

## 2. Method and tip/surface setup

The calculations were performed using the linear combination of atomic orbitals (LCAO) basis SIESTA

code [17,18], implementing the density functional theory (DFT) with the generalised gradient approximation (GGA) and the functional of Perdew, Burke and Ernzerhof known as PBE [19]. Core electrons are represented by norm-conserving pseudopotentials using the Troullier–Martins parameterisation [18]. The pseudopotential for the silicon atom was generated in the electron configuration  $[\text{Ne}]3s^23p^2$ , for calcium in  $[\text{Ar}]4s^2$ , carbon in  $[1s^2]2s^22p^2$ , oxygen in  $[1s^2]2s^22p^4$ , fluorine in  $[1s^2]2s^22p^5$ , and that for magnesium in  $[\text{Ne}]3s^2$  configuration, where square brackets denote the core electron configurations.

To simulate a silicon tip with a single dangling bond at the apex, we use a 10-atom silicon cluster, with its base terminated by hydrogen [20], as shown in Fig. 1(a). The small size, specific shape and hydrogen termination of the tip produce a surface electronic structure different from a standard silicon surface. However, since a real AFM tip is also very different from a standard silicon surface, this represents a fair approximation. The highest occupied molecular orbital (HOMO) of the tip, representing the dangling bond, is shown in Fig. 1(b). One can see that it is quite diffuse and will overlap simultaneously with several surface ions. The corresponding one-electron state is split from other occupied states of the Si tip modelling the Si valence band. This state can be seen at the Fermi energy in Fig. 2.

The surface structures of the three crystals considered in this paper are shown in Fig. 3. They have been

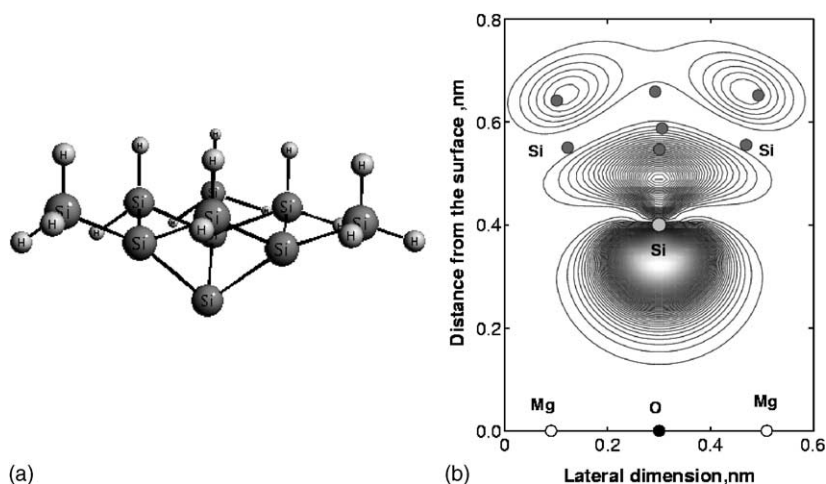


Fig. 1. (a) Silicon tip used in this study. (b) Contour density plot (100 levels with  $0.002 \text{ Bohr}^{-3}$  step) of HOMO orbital associated with dangling bond of Si cluster.

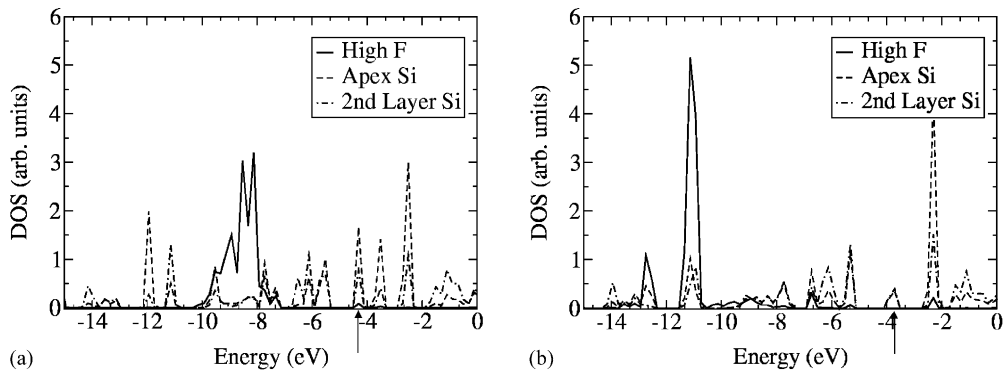


Fig. 2. Partial densities of states for the surface high F atom, and silicon atoms at the apex and in the second layer of the tip with the tip at: (a) 0.4 nm and (b) 0.25 nm over the high F in the  $\text{CaF}_2$  surface. The arrows mark the position of the Fermi energy.

discussed in detail in Ref. [16]. The  $\text{CaF}_2(1\ 1\ 1)$  surface is fluorine terminated, with a substructure seen in Fig. 3(a). For convenience, in further discussion we will denote the fluorine ions in the upper surface layer—‘high’  $\text{F}^-$  ions and those in the third surface layer—‘low’  $\text{F}^-$  ions. The distance between unrelaxed tip apex and unrelaxed uppermost surface sublattice is used as a reference for measuring the tip–surface height in all calculations. The  $\text{CaF}_2$  crystal surface is here simulated by a periodic cell of  $(4 \times 4 \times 3)$   $\text{CaF}_2$  units. The calculated electronic bandgap of this system is equal to 6.6 eV, which is almost half the bulk experimental value of 12.1 eV.

The  $(1\ 0\ \bar{1}\ 4)$  calcite surface is interesting since it is a very low symmetry ionic system, where one ionic species is  $\text{Ca}^{2+}$  and another is a covalently bound molecular group, namely  $\text{CO}_3^{2-}$ . The main features of

this complex surface are schematically depicted in Fig. 3(b). The surface unit cell is composed of two  $\text{Ca}^{2+}$  ions and two  $\text{CO}_3^{2-}$  groups, where the calcium ions define a surface parallel plane that also contains carbon atoms. Only one oxygen atom of each group shares this plane while the two others are located above and below. The groups appear in two different orientations with respect to a rotation around an axis perpendicular to the surface plane. Therefore, neighbouring rows of groups along the  $[0\ 1\ 0]$  direction are not equivalent and the most protruding oxygen atoms form a zigzag structure oriented in the  $[\bar{4}\ \bar{2}\ 1]$  direction. This surface was modelled by a slab containing  $(3 \times 4 \times 3)$   $\text{CaCO}_3$  units. The calculated electronic structure confirms the qualitative model described above with effective Mulliken charges on the surface  $\text{Ca}^{2+}$  ions equal to  $+1.8e$ . The calculated surface

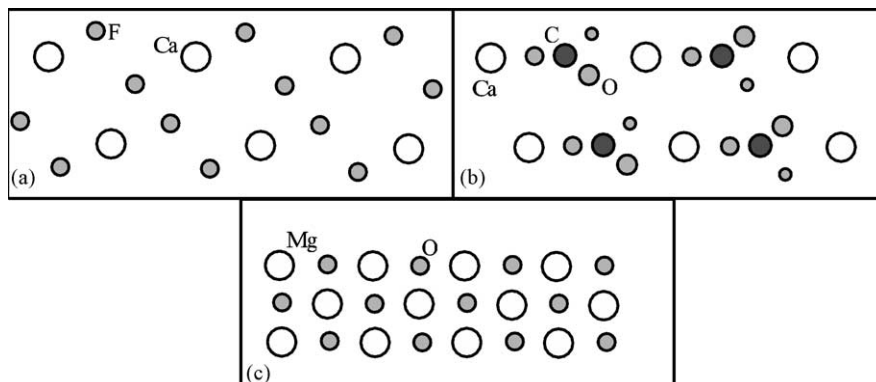


Fig. 3. Side cross-sections in the  $x$ - $z$  plane of the atomic structures of surfaces considered in this study: (a)  $\text{CaF}_2(1\ 1\ 1)$ , (b)  $\text{CaCO}_3(1\ 0\ \bar{1}\ 4)$  and (c)  $\text{MgO}(0\ 0\ 1)$ . Note that the oxygen atoms in  $\text{CaCO}_3$  have been drawn in perspective.

bandgap is equal to 5.0 eV which is again smaller than the experimental bulk value of 6.0 eV.

Finally, the MgO(0 0 1) surface shown in Fig. 3(c) is a relatively much more simple termination of an f.c.c. structure. Its properties and surface rumpling have been studied in many previous DFT calculations (see, for example, Ref. [21]) and are well reproduced in the present work using the SIESTA code. The surface was modelled using a slab with the  $(6 \times 3 \times 3)$  MgO units. The calculated bandgap is equal to 3.6 eV, which is much smaller than the bulk experimental value of 7.8 eV.

The systematically narrow bandgaps noted above are a characteristic feature of standard DFT methods based on local functionals. Parameters of the electronic structure important for the purpose of the present study are the energy offsets between the top of the valence bands of the crystals under study and the top of the Si valence band. These values for large tip–surface separations are 1.8,  $-0.8$  and  $-1.3$  eV for CaF<sub>2</sub>, CaCO<sub>3</sub>, and MgO, respectively. The negative values mean that the top of Si valence band is lower than that of the insulator. Correspondingly, the offset with the dangling bond state and with the unoccupied Si states is the largest for the CaF<sub>2</sub> crystal surface and the smallest for MgO. Although this trend is qualitatively right, the value of the offset is most probably underestimated. In particular, the band offset calculated for the Si/CaF<sub>2</sub> planar interface using a similar method is around 6 eV, whereas the experimental value is around 8 eV [12]. The value of the offset is affected both by the inaccuracy of the method of calculation and by the difference between the planar Si surface geometry and the tip structure. Nevertheless, we believe that the general features predicted in these calculations are correct.

Modelling of the tip–surface interaction in a periodic slab model implies periodic repetition of the tip along the surface and hence the tip–tip interaction. The characteristic distance between tips periodically translated along the surface in our calculations is about 0.3 nm. The gap between slabs in the direction perpendicular to the surface is about 4 nm. The bottom two layers of the tip and the top two layers of the surfaces were allowed to relax with respect to atomic forces. This provides a good estimate of the tip and surface deformation due to their interaction.

Finally, we should note that most of the calculations were performed using a non-spin-polarised version of the DFT method. By comparing with the spin-polarised calculation of the Si tip we have checked that this does not affect significantly the tip electronic structure or tip–surface forces. All calculations involving the geometry optimisation were performed in the gamma point of the Brillouin zone, then repeated with two or more  $k$  points to obtain more accurate electronic structure and density of states.

### 3. The tip–surface interaction

The tip–surface interaction was calculated for a number of distances above the surface sites. Qualitatively, in all cases we find an electron density redistribution from surface anions to the Si tip, which is stronger when the tip is directly above the outmost surface fluorine or oxygen ion. However, due to the diffuse character of the dangling bond orbital (see Fig. 1(b)) a smaller electron redistribution from anions takes place at other tip positions too. The amount of the electron density transferred from the surface occupied states into the tip unoccupied states increases as the band offset decreases, and is generally largest for the MgO case. It can be qualitatively characterised using Mulliken population analysis [22]. The calculated values of charges transferred to the tip when it was at 0.40 and 0.25 nm directly above anions of the all three surfaces considered in this paper are given in Table 1. If no charge is transferred, the tip–surface interaction would be only due to the tip polarisation by the electric field produced by ionic surfaces. This is

Table 1  
Data for a silicon tip interacting with the three systems studied<sup>a</sup>

Material	Displacement of anion (Å)	Charge transfer from anion, $e$	Force (eV/Å)
CaF <sub>2</sub>	+0.00 (+0.13)	$-0.01$	$-0.09$ ( $-0.15$ )
CaCO <sub>3</sub>	+0.01 (+0.22)	$-0.02$	$-0.03$ ( $-0.23$ )
MgO	+0.05 (+0.18)	$-0.05$	$-0.36$ ( $-0.19$ )
CaF <sub>2</sub>	+0.40 (+0.50)	$-0.20$	$-0.55$ ( $-0.29$ )
CaCO <sub>3</sub>	+0.46 (+0.34)	$-0.24$	$-1.10$ ( $-0.51$ )
MgO	+0.19 (+0.32)	$-0.21$	$-0.73$ ( $-0.42$ )

<sup>a</sup> The tip height in the first three rows are taken at 0.400 nm above the highest anion of the surface and the second three rows at 0.250 nm. Values in brackets are for a positive potential MgO tip.

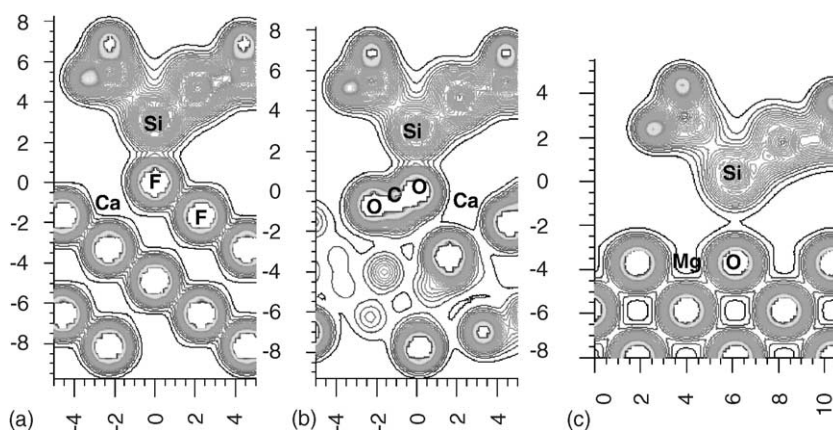


Fig. 4. Charge density plots in the  $x$ - $z$  plane through the tip apex and the anion under the tip at a height of 0.4 nm over the surface of: (a) CaF<sub>2</sub>, (b) CaCO<sub>3</sub> and (c) MgO; distances are in Å.

the situation at a height of 0.4 nm, where it is clear from Table 1 that the ionic tip produces a stronger force and much larger displacements of the anion under the tip. Note, however, that for MgO the charge transfer and displacements for a silicon tip are double in comparison to the other surfaces at 0.4 nm. At closer range we see the onset of stronger covalent bonding between Si and the surface fluorine and oxygen ions. This can be clearly seen in the sections of the electron density plots presented in Fig. 4. Evidence of this bonding can also be seen in the example partial densities of states in Fig. 2, where there are large changes in the dangling bond and anion states as the tip approaches. Table 1 shows that at 0.25 nm the force acting on the silicon tip is larger than that found for the ionic MgO tip, and displacements for the two types of interaction are comparable.

A more detailed analysis of the calculated tip-surface forces as the silicon tip approaches the Ca<sup>2+</sup>, high F<sup>-</sup> and low F<sup>-</sup> sublattices in the CaF<sub>2</sub> surface demonstrates that contrast in images with a silicon tip would be dominated by interaction with the high F<sup>-</sup> sublattice, and to a lesser extent the low F<sup>-</sup> sublattice. The interaction with Ca<sup>2+</sup> is much weaker, and enters repulsion at about 0.33 nm. The stronger interaction between the tip and the F<sup>-</sup> ions is due to the onset of covalent bonding, involving electron redistribution from the F<sup>-</sup> ions into bonding states. At 0.375 nm tip height, charge transfer is 0.18 $e$  for the high F<sup>-</sup>, but only 0.02 $e$  for the low F<sup>-</sup>. Over Ca, there is no charge transfer until small heights (about 0.30 nm), where

electron density is actually transferred from the neighbouring high F<sup>-</sup> site to the tip (see Fig. 4(a)).

At smaller ranges, the force for the ionic tip is strongly influenced by large displacements of surface ions induced by the tip approach. However, for the silicon tip, until very close range, interaction forces are considerably smaller than for the ionic tip and, therefore, displacements are much smaller. Over the Ca<sup>2+</sup> ions, there is almost no surface ion displacement until very small tip-surface separations when the Ca<sup>2+</sup> directly underneath the tip is pushed in. Over the high F<sup>-</sup>, at 0.250 nm the F<sup>-</sup> ion under the tip is at a maximum displacement of 0.040 nm towards the tip, before being pushed back in. There is no significant displacement of the low F<sup>-</sup>, or any atoms not directly underneath the tip.

Similar analysis of the interaction with the calcite surface demonstrates stronger electron redistribution, and more complex surface atomic relaxation. Although Table 1 indicates that charge transfer for CaF<sub>2</sub> and calcite is similar, in fact, charge transfer occurs from the whole carbonate group, rather than a single ion, and is approximately twice larger than for CaF<sub>2</sub>.

Relaxations are also more complex, with the carbonate group displacing as a unit due to the very strong covalent bonds between C and O atoms. Over the Ca<sup>2+</sup> ions, displacements are very small until close approach when the ion is driven into the surface, similar to CaF<sub>2</sub>. However, over the C atom, the carbon initially displaces towards the tip, with a maximum of +0.011 nm at 0.250 nm tip height, but it is then

pushed back into  $-0.038$  nm at  $0.125$  nm as the tip feels strong repulsion from the nearby high oxygen. Similar, but more extreme behaviour is seen over the high oxygen itself, with a maximum outward displacement of  $+0.034$  nm at  $0.250$  nm, and then  $-0.038$  at  $0.125$  nm. However, for the middle oxygen, the high oxygen does not interfere and repel the tip, and the atom displaces only out of the surface to a maximum of  $+0.041$  nm at  $0.175$  nm tip height. Finally, over the low oxygen the displacements are much smaller, with only an inward shift of  $-0.026$  nm at  $0.125$  nm. This is once again mainly due to repulsion of the tip with the high oxygen, and emphasises that the elements of the carbonate group are interconnected, and therefore no atom is moving independently.

Finally we note that due to the softness of the silicon tip in comparison to the ionic MgO tip, tip atom relaxations play a more significant role in these interactions. For example, over calcite the apex silicon relaxes by up to  $0.057$  nm away from the surface.

#### 4. Conclusions

We have studied the interaction of a model Si tip with the surfaces of wide-gap insulators  $\text{CaCO}_3$ , MgO, and  $\text{CaF}_2$ . The results demonstrate that the strength of this interaction is largely determined by the extent of the electron density redistribution between the surface anions (which determine the top of the surface valence band) and the tip. The latter, in its turn, depends on the offset of the surface and tip valence bands and is larger for smaller offsets characteristic for calcite and MgO.

Comparing the magnitude of force curves for Si and ionic MgO tips for the  $\text{CaF}_2(1\ 1\ 1)$  surface, studied in detail both experimentally and theoretically [23], we conclude that the force between a pure silicon tip and the  $\text{CaF}_2$  surface is much less than for positive potential ionic tip. If we calculate the maximum possible contrast for a pure silicon tip imaging  $\text{CaF}_2$  it is about 2 Hz—several times smaller than that seen for simulations with an ionic tip, and, more significantly, in experiments [24]. A stronger contrast is expected in the case of calcite and MgO surfaces where the tip–surface interaction with the model Si tip at short tip–surface separations is similar and even stronger than that with the fully ionic MgO tip. These results provide yet another example of the strong dependence

of the tip–surface interaction, and hence image contrast on the chemical nature of the tip apex.

Since the degree of the electron density redistribution depends on the relative position of the tip and surface electronic states, it can be affected by the voltage applied between the tip and conductive substrate or sample holder. In particular, recent experiments by Shimizu et al. [25] have demonstrated that by measuring attractive forces between an insulating sample and a metal coated tip as a function of applied voltage between tip and conductive substrate, one can determine the electron bandgap of the surface material. Further studies of the dependence of the interaction of conducting tips with insulators may open new avenues for controlling the strength of the tip–surface interaction and studying the surface electronic structure.

#### Acknowledgements

ASF is grateful to the Centre for Scientific Computing, Helsinki, for use of its computational resources. AYG would like to thank EPSRC for financial support. We are grateful to M. Reichling, C. Barth, R. Hoffman and F. Giessibl for stimulating discussions, and J. Gale for help with the SIESTA code.

#### References

- [1] A.I. Livshits, A.L. Shluger, A.L. Rohl, A.S. Foster, *Phys. Rev. B* 59 (1999) 2436.
- [2] R. Pérez, M. Payne, I. Stich, K. Terakura, *Phys. Rev. Lett.* 78 (1997) 678.
- [3] M.A. Lantz, H.J. Hug, P.J.A. van Schendel, R. Hoffman, S. Martin, A. Baratoff, A. Abdurixit, H.J. Güntherodt, C. Gerber, *Phys. Rev. Lett.* 84 (2000) 2642.
- [4] M.A. Lantz, H.J. Hug, R. Hoffman, P.J.A. van Schendel, P. Kappenberger, S. Martin, A. Baratoff, H.J. Güntherodt, *Science* 291 (2001) 2580.
- [5] J. Tóbiš, I. Stich, R. Pérez, K. Terakura, *Phys. Rev. B* 60 (1999) 11639.
- [6] S.H. Ke, T. Uda, R. Pérez, I. Stich, K. Terakura, *Phys. Rev. B* 60 (1999) 11631.
- [7] S.H. Ke, T. Uda, K. Terakura, *Phys. Rev. B* 65 (2002) 125417.
- [8] J.G. Li, *Mater. Chem. Phys.* 47 (1997) 126.
- [9] B. Ealet, E. Gillet, *Surf. Sci.* 367 (1996) 221.
- [10] M.W. Finnis, *J. Phys.: Condens. Matter* 8 (1996) 5811.
- [11] P. Avouris, R. Wolkow, *Appl. Phys. Lett.* 55 (1989) 1074.
- [12] M.R. Salehpour, S. Satpathy, *Phys. Rev. B* 44 (1991) 8880.

- [13] H. Hosoi, K. Sueoka, K. Hayakawa, K. Mukasa, *Appl. Surf. Sci.* 157 (2000).
- [14] W. Allers, S. Langkat, R. Wiesendanger, *Appl. Phys. A* 72 (2001) S27.
- [15] F.J. Giessibl, S. Hembacher, H. Bielefeldt, J. Mannhart, *Science* 289 (2000) 422.
- [16] S. Morita, R. Wiesendanger, E. Meyer (Eds.), *Noncontact Atomic Force Microscopy*, Springer, Berlin, 2002.
- [17] J. Junquera, O. Paz, D. Sánchez-Portal, E. Artacho, *Phys. Rev. B*, in press.
- [18] J.M. Soler, E. Artacho, J.D. Gale, A. García, J. Junquera, P. Ordejón, D. Sánchez-Portal, *J. Phys.: Condens. Matter* 14 (2002) 2745.
- [19] J.P. Perdew, K. Burke, M. Ernzerhof, *Phys. Rev. Lett.* 77 (1996) 3865.
- [20] R. Pérez, I. Stich, M. Payne, K. Terakura, *Phys. Rev. B* 58 (1998) 10835.
- [21] L.N. Kantorovich, J.M. Holender, M.J. Gillan, *Surf. Sci.* 343 (1997) 221.
- [22] R.S. Mulliken, *J. Chim. Phys.* 49 (1949) 497.
- [23] A.S. Foster, C. Barth, A.L. Shluger, R.M. Nieminen, M. Reichling, *Phys. Rev. B* 66 (2002) 235417.
- [24] C. Barth, A.S. Foster, M. Reichling, A.L. Shluger, *J. Phys.: Condens. Matter* 13 (2001) 2061.
- [25] M. Shimizu, H. Watanabe, K. Anazawa, T. Miyahara, C. Manabe, *J. Chem. Phys.* 110 (1999) 12116.